Fluid pulsation modes and tidal deformability of anisotropic strange stars in light of the GW170817 event

José D. V. Arbañil,[1,2,*] Cesar V. Flores,[3,4,†] César H. Lenzi,[5,‡] and Juan M. Z. Pretel[6,§]

[1]*Departamento de Ciencias, Universidad Privada del Norte, Avenida el Sol 461 San Juan de Lurigancho, 15434 Lima, Peru*
[2]*Facultad de Ciencias Físicas, Universidad Nacional Mayor de San Marcos, Avenida Venezuela s/n Cercado de Lima, 15081 Lima, Peru*
[3]*Departamento de Física-CCET, Universidade Federal do Maranhão, Campus Universitário do Bacanga, São Luís CEP 65080-805, MA, Brazil*
[4]*Centro de Ciências Exatas, Naturais e Tecnológicas, Universidade Estadual da Região Tocantina do Maranhão, Imperatriz CEP 65901-480, Maranhão, Brazil*
[5]*Departamento de Física, Instituto Tecnológico de Aeronáutica, Centro Técnico Aeroespacial, 12228-900 São José dos Campos, São Paulo, Brazil*
[6]*Centro Brasileiro de Pesquisas Físicas, Rua Dr. Xavier Sigaud, 150 URCA, Rio de Janeiro CEP 22290-180, Rio de Janeiro, Brazil*

(Received 13 April 2023; accepted 22 May 2023; published 9 June 2023)

The effects of anisotropy on the fluid pulsation modes when adopting the so-called Cowling approximation and the tidal deformability of strange-quark stars are investigated by numerically integrating the hydrostatic equilibrium, nonradial oscillation, and tidal deformability equations, all of which are modified from their standard form to include the anisotropic effects. The fluid matter inside compact stars is described by the MIT bag model equation of state. For the anisotropy profile, we consider a local anisotropy that is both regular at the center and null at the star's surface. We find that the effect of anisotropy is reflected in the fluid pulsation modes and tidal deformability. Finally, we analyze the correlation between the tidal deformability of the GW170817 event and anisotropy.

DOI: 10.1103/PhysRevD.107.124016

I. INTRODUCTION

With all of the recent detections of gravitational signals coming from the mergers of binary systems reported by the LIGO/Virgo Collaboration (LVC) [1–10], we can say that we live at the beginning of a new golden age in general relativity: the age of gravitational-wave astronomy. In this sense, it is essential to invest our best efforts in order to study new quantitative, qualitative, and even exotic physical characteristics that could be present in future multi-messenger observations.

Among these phenomena, it is well known that compact stars can be present as components of binary systems. Thus, the behavior of a compact star before, during, and after the merger cannot be ignored. For example, when when binaries are very close to each other, tidal interactions play an important role [10], and this could be a natural route to obtain information about the equation of state (EOS) from the signals emitted during the merger of two compact stars.

The theoretical methods of asteroseismology are used to investigate the oscillation frequencies of stars. This theory is a powerful tool that gives us a firm path in the search for traces of physics inside compact stars [11–14]. In this way, the oscillation frequencies of such stars, namely, f- and p-modes [15,16], would give us information about the composition and internal structure of such spherical objects (see, e.g., Refs. [17–21] and references therein).

An important aspect to be analyzed in the study of compact objects is the tidal deformability [22–26]. As previously mentioned, this parameter gives us information about the EOS hidden in the signals emitted by compact stars. Moreover, nowadays, using dimensionless tidal deformability, we can place some limits on the theory using the observational data of the event GW170817.

In this regard, we investigate the nonradial oscillation modes and tidal deformability of anisotropic strange-quark stars. As reported, theoretical evidence indicates that anisotropies can emerge in highly dense media, such as that appearing in phase transitions [27], the pion condensed phase [28], a solid or superfluid nucleus [29,30], or in the presence of superfluid ^{3}He-A [31]. Since establishing a connection between the internal composition of the compact star and the results reported by observation has been the

*jose.arbanil@upn.pe
†cesarovfsky@gmail.com
‡chlenzi@ita.br
§juanzarate@cbpf.br

purpose of many works, the tidal deformability results found in this work are analyzed in light of the deformability parameter obtained from the event GW170817; see Ref. [32].

This article is structured as follows. In Sec. II we present the Einstein field equation, energy-momentum tensor, stellar structure equations, nonradial oscillation equations, and tidal deformability equations and their boundary conditions. In Sec. III we show the numerical method employed, the EOS, the anisotropic profile, and the scaling solution for nonradial oscillation equations and tidal deformability equations. Moreover, we plot the change of the oscillation frequency and tidal deformability against anisotropy. Finally, we conclude in Sec. IV. Throughout the paper, in order to simplify our equations and also for numerical reasons, we employ the units $G = 1 = c$.

II. GENERAL-RELATIVISTIC FORMULATION

A. Einstein field equation

We start by writing the Einstein field equation in the presence of an anisotropic fluid:

$$G^{\mu}_{\varphi} = 8\pi T^{\mu}_{\varphi}, \tag{1}$$

where the greek indexes μ, φ, etc., go from 0 to 3, G^{μ}_{φ} is the Einstein tensor, and T^{μ}_{φ} represents the energy-momentum tensor which is given by

$$T^{\mu}_{\varphi} = (\rho + p_t)u^{\mu}u_{\varphi} + p_t g^{\mu}_{\varphi} - \sigma k^{\mu}k^{\nu}g_{\nu\varphi}, \tag{2}$$

with ρ, p_t, and $\sigma = p_t - p_r$ are, respectively, the energy density, tangential pressure, and anisotropic pressure parameter, where p_r is the radial pressure. In addition, u_{φ} is the four-velocity of the fluid, k_{φ} denotes the radial unit vector, and $g_{\mu\varphi}$ is the metric tensor. These four-vectors must satisfy the following conditions:

$$k_{\varphi}k^{\varphi} = 1, \qquad u_{\varphi}k^{\varphi} = 0, \qquad u_{\varphi}u^{\varphi} = -1. \tag{3}$$

B. Static background equations

The unperturbed spherically symmetric line element, in Schwarzschild-like coordinates, is expressed in the form

$$ds^2 = -e^{2\Phi}dt^2 + e^{2\Psi}dr^2 + r^2(d\theta^2 + \sin^2\theta d\phi^2), \tag{4}$$

where the metric functions $\Phi = \Phi(r)$ and $\Psi = \Psi(r)$ depend on the radial coordinate r alone.

Considering the spacetime metric (4) and the potential metric

$$e^{-2\Psi} = \left(1 - \frac{2m}{r}\right), \tag{5}$$

the non-null components of the field equations (1) can be placed into the form

$$m' = 4\pi\rho r^2, \tag{6}$$

$$p_r' = -(p_r + \rho)\left[4\pi r p_r + \frac{m}{r^2}\right]e^{2\Psi} + \frac{2\sigma}{r}, \tag{7}$$

$$\Phi' = -\frac{p_r'}{\rho + p_r} + \frac{2\sigma}{r(\rho + p_r)}. \tag{8}$$

The function $m(r)$ is the mass enclosed within the sphere radius r. Equations (6) and (7) represent, respectively, the mass conservation and the hydrostatic equilibrium equation [33,34] modified from the original form to include the anisotropic factor [35]. This set of equations is known as the stellar structure equations. A prime ($'$) over a functions represents a derivative with respect to r.

To obtain the stellar equilibrium configurations, we integrate Eqs. (6)–(8) from the origin up to the radial coordinate where the radial pressure vanishes. In other words, the solution starts at the center of the star ($r = 0$), where

$$m(0) = 0, \quad \Psi(0) = 0, \quad \Phi(0) = \Phi_c, \quad \rho(0) = \rho_c, \tag{9}$$

and the stellar surface ($r = R$) is determined by

$$p_r(R) = 0. \tag{10}$$

In addition, at $r = R$, the interior spacetime metric connects smoothly with the Schwarzschild vacuum exterior solution, so that

$$e^{2\Phi} = e^{-2\Psi} = 1 - \frac{2M}{R}, \tag{11}$$

where M is the total mass of the star.

C. Nonradial oscillation equations within the Cowling approximation

In non-radial oscillations of compact stars, the Cowling formalism [36,37] is often used to calculate the oscillation frequencies (see, for example, Refs. [38,39]). This method provides a good precision of the oscillation frequencies obtained from by relativistic numerical approach. In fact, in typical stellar models, discrepancies of less than 20% and 10% for the f- and p_1-modes are found between these methods, respectively [40]. This good precision justifies its use to study, for example, the fluid pulsation mode of neutron stars in the presence of slow [41] and rapid rotation rates [42], crust elasticity [43], internal anisotropy [44], and d dimensions [45].

To investigate pulsation modes of anisotropic strange stars, the metric functions are kept fixed in the Cowling approximation, i.e., $\delta g_{\mu\nu} = 0$ [39]. In addition, the equations describing the fluid pulsation are obtained by perturbing the conservation equation of the energy-momentum tensor (2). Hence, we obtain $\delta(\nabla_\mu T^{\mu\nu}) = 0$. Projecting this relation both along the four-velocity u_ν and orthogonally by employing the operator $\mathcal{P}^\nu_\mu = \delta^\nu_\mu + u^\nu u_\mu$, we get, respectively,

$$u^\nu \nabla_\nu \delta\rho + \nabla_\nu([(\rho + p_t)\delta^\nu_\mu - \sigma k^\nu k_\mu]\delta u^\mu) + (\rho + p_t) a_\nu \delta u^\nu - \nabla_\nu u_\mu \delta(\sigma k^\nu k^\mu) = 0, \tag{12}$$

$$(\delta\rho + \delta p_t) a_\mu + (\rho + p_t) u^\nu (\nabla_\nu \delta u_\mu - \nabla_\mu \delta u_\nu) + \nabla_\mu \delta p_t + u_\mu u^\nu \nabla_\nu \delta p_t - \mathcal{P}^\nu_\mu \nabla_\alpha \delta(\sigma k^\alpha k_\nu) = 0, \tag{13}$$

with $a_\mu = u^\nu \nabla_\nu u_\mu$ being the four-acceleration.

We take the Lagrangian fluid vector components into account in the form

$$\xi^i = \left(e^{-\Psi} W, -V\partial_\theta, -\frac{V}{\sin^2\theta}\partial_\phi\right)\frac{Y_{\ell m}}{r^2}, \tag{14}$$

with $W = W(t, r)$ and $V = V(t, r)$ being functions of the coordinates t and r, and $Y_{\ell m} = Y_{\ell m}(\theta, \phi)$ are the spherical harmonics. In such a way, the perturbation of the four-fluid through the Lagrangian perturbation vector $\delta u^\mu = (0, \delta u^r, \delta u^\theta, \delta u^\phi)$ can be expressed as

$$\delta u^\mu = \left(0, e^{-\Psi}\partial_t W, -\partial_t V\partial_\theta, -\frac{\partial_t V}{\sin^2\theta}\partial_\phi\right)\frac{Y_{\ell m} e^{-\Phi}}{r^2}. \tag{15}$$

Considering $u^\mu = (e^{-\Phi}, 0, 0, 0)$, $k^\mu = (0, e^{-\Psi}, 0, 0)$, $\sigma = \sigma(p_r, \mu)$, $W(t, r) = W(r)e^{i\omega t}$, and $V(t, r) = V(r)e^{i\omega t}$ in Eqs. (12) and (13), we arrive at the following system of equations:

$$W' = \frac{d\rho}{dp_r}\left[(1 + \mathcal{X})\left(1 + \frac{\partial\sigma}{\partial p_r}\right)^{-1}\frac{\omega^2 r^2 V}{e^{2\Phi-\Psi}} + \Phi' W\right] - \mathcal{X}\left[\left(1 + \frac{d\rho}{dp_r}\right)\frac{2W}{r} + \ell(\ell+1)e^{\Psi}V\right] - \ell(\ell+1)e^{\Psi}V, \tag{16}$$

$$V' = V\left[-\frac{\sigma'}{\rho + p_r + \sigma} - \left(\frac{d\rho}{dp_r} + 1\right)\left(\Phi' + \frac{2}{r}\right)\frac{\mathcal{X}}{1 + \mathcal{X}} + \frac{2}{r}\frac{\partial\sigma}{\partial p_r} + \left(1 + \frac{\partial\sigma}{\partial p_r}\right)^{-1}\left(\frac{\partial^2\sigma}{\partial p_r^2}p_r' + \frac{\partial^2\sigma}{\partial p_r\partial\mu}\mu'\right)\right] + 2V\Phi' - \left(1 + \frac{\partial\sigma}{\partial p_r}\right)\frac{1}{1 + \mathcal{X}}\frac{e^{\Psi}W}{r^2}, \tag{17}$$

where we have defined $\mathcal{X} = \sigma/(\rho + p_r)$ and, following Ref. [44], we consider $\delta\sigma = (\partial\sigma/\partial p_r)\delta p_r$, with $\delta\mu = 0$ ($\mu = 2m/r$), and ω represents the oscillation eigenfrequency. These two differential equations are reduced to those found in Ref. [39] taking $\sigma = 0$.

To solve Eqs. (16) and (17) from the center ($r = 0$) toward the stellar surface ($r = R$), we need to impose boundary conditions. Thus, at $r = 0$ we consider that the functions W and V assume the respective forms

$$W = Cr^{\ell+1}, \qquad V = -C\frac{r^\ell}{\ell}, \tag{18}$$

with C representing a dimensionless constant. Moreover, at $r = R$ (where $p_r = 0$) we find

$$[1 + \mathcal{X}]\frac{\omega^2 V}{e^{2\Phi}} + \left[1 + \frac{\partial\sigma}{\partial p_r}\right]\left[\frac{r\Phi'}{2} - \mathcal{X}\right]\frac{2W}{e^{\Psi}r^3} = 0. \tag{19}$$

Hereafter, to compare our results with those shown in the literature (e.g., Refs. [44,46]), we restrict our results to the quadrupolar modes ($\ell = 2$).

D. Tidal deformability

The theory of tidal Love numbers is frequently studied within the context of binary compact star systems. In this scheme, the gravitational effects caused by one star can result in the deformation of its companion. Such deformation, produced by an external field, can be measured through the tidal deformability parameter λ. This parameter can be expressed as follows:

$$\lambda = -\frac{Q_{ij}}{\epsilon_{ij}}, \tag{20}$$

with Q_{ij} and ϵ_{ij} representing the quadrupole moment and an external tidal field; see Refs. [24,26,47]. The relation that directly connects the tidal deformability parameter and the quadrupolar Love number k_2 is given by

$$k_2 = \frac{3}{2}\lambda R^{-5}. \tag{21}$$

Furthermore, the dimensionless tidal deformability Λ, as a function of the Love number k_2, follows from the following relation:

$$\Lambda = \frac{2k_2}{3C^5}, \tag{22}$$

where $C = M/R$ represents the compactness parameter. k_2 can also be written in terms of C. Thus, we have

$$k_2 = \frac{8C^5}{5}(1 - 2C)^2[2 + C(y_R - 1) - y_R] \times \{2C[6 - 3y_R + 3C(5y_R - 8)] + 4C^3[13 - 11y_R + C(3y_R - 2) + 2C^2(1 + y_R)] + 3(1 - 2C^2) \times [2 - y_R + 2(y_R - 1)]\ln(1 - 2C)\}^{-1}, \tag{23}$$

with the function $y_R = y(r = R)$. In addition, the function $y(r)$ satisfies the Riccati differential equation

$$y'r + y^2 + y(C_0 r - 1) + C_1 r^2 = 0, \tag{24}$$

where

$$C_0 = \frac{2m}{r^2} e^{2\Psi} + 4\pi e^{2\Psi}(p_r - \rho)r + \frac{2}{r}, \tag{25}$$

$$C_1 = 4\pi e^{2\Psi}\left[4\rho + 4p_r + 4p_t + \frac{p_r + \rho}{Ac_s^2}(c_s^2 + 1)\right] - \frac{6}{r^2}e^{2\Psi} - 4\Phi'^2, \tag{26}$$

with $c_s^2 = \frac{dp_r}{d\rho}$ and $A = \frac{dp_t}{dp_r}$. Comparing Eqs. (25) and (26) with the forms presented in Refs. [48,49], we see that our C_0 and C_1 are in agreement and contradiction, respectively, with those presented in these two works. Note that the first-order differential equation (24) is derived from the second-order differential equation for the function H in the quadrupolar case ($\ell = 2$), Eq. (A11), by using $y = rH'/H$. Moreover, if we consider $p_t = p_r$ (i.e., $A = 1$), Eq. (24) is reduced to the isotropic case (see Ref. [25]).

In particular, for strange-quark stars—where the energy density at the star's surface is finite and non-null—a correction term is required in the calculation of y_R. Thus, due to this energy discontinuity y_R is [26,50–53]

$$y_R \to y_R - \frac{4\pi R^3 \rho_s}{M}, \tag{27}$$

where ρ_s represents the energy density difference between the internal and external regions.

III. RESULTS

A. Numerical method

To investigate the influence of anisotropy in the oscillation spectrum and tidal deformability of strange stars—once defined the EOS and the anisotropic profile—the stellar structure equations (5)–(7), the nonradial oscillation equations (16) and (17), and the tidal deformability equations (22)–(26) are integrated from the center ($r = 0$) to the star's surface ($r = R$).

To study both the fluid perturbation modes and the tidal deformability, we first integrate Eqs. (5)–(8) from the center to the star's surface using the fourth-order Runge-Kutta method, for different values of κ and ρ_c. Once we determine the parameters p_r, p_t, ρ, m, and Φ, Eq. (8) is solved using the shooting method. This integration begins by considering a proof value of Φ_c; if after the numerical integration the equality shown in Eq. (11) is not attained, Φ_c is corrected until it satisfies this condition.

The numerical solution of the nonradial oscillations and tidal deformability equations are described below:

(1) The fluid perturbation modes equations [Eqs. (16) and (17)] are integrated from the center to the star's surface. The process begins by taking into account the correct value of Φ_c in the stellar structure equations for particular values of κ and ρ_c and the test value of ω^2. If the numerical integration of the equality (19) is not reached, ω^2 is corrected in the next integration until this condition is satisfied.

(2) The tidal deformability equations [Eqs. (22)–(26)] are integrated along the radial coordinate r which goes from 0 to R. It starts employing the correct value of Φ_c in the stellar structure equations for a particular value of κ and ρ_c.

B. Equation of state and anisotropic profile

To depict the strange-quark fluid that makes up the compact object, the MIT bag model EOS is employed. This EOS describes a fluid containing only up, down, and strange quarks that have no mass and no interaction, confined by a bag constant $\mathcal{B}$. For the anisotropic fluid analyzed here, we assume that the radial pressure and the energy density are related by the equality

$$p_r = \frac{1}{3}(\rho - 4\mathcal{B}). \tag{28}$$

This EOS is widely employed by different authors since Witten proposed that strange matter can be the ground state of strongly interacting matter and it could appear in compact stars [54]. In Ref. [55] this hypothesis was verified for a bag constant in the range of 57 to 94 $\mathrm{MeV/fm^3}$. Following Ref. [56], we employ $\mathcal{B} = 60\ \mathrm{MeV/fm^3}$.

For the anisotropic pressure profile, inspired by Refs. [44,56–60], we use the quasilocal form $\sigma = \sigma(p_r, \Psi)$. It depends on quantities that provide information on both the state of the fluid and the geometry at a particular interior point of the spacetime. Thus, we consider the anisotropic profile

$$\sigma = \kappa p_r (1 - e^{-2\Psi}), \tag{29}$$

where κ is a dimensionless anisotropic constant. The relation (29) was used, for instance, to investigate the influence of the anisotropy on the radial oscillation of polytropic stars [57,58] and strange stars [56], the nonradial oscillation of neutron stars [44], magnetic field structure [59], and slowly rotating neutron stars [60].

C. Scaling solution of nonradial oscillation equations and tidal deformability equations

In the literature, it has been reported that when a linear EOS is used to describe the fluid of a star, e.g., the MIT bag model EOS, both the stellar structure and radial oscillation equations admit a scaling law for several star properties [54,56,61]. This means that if a star's properties are known for a given $\mathcal{B}$, these properties can be found for another value $\mathcal{B}'$.

For stellar structure, nonradial oscillation, and tidal deformability equations a scaling law can also be used. This can be realized through the following variables:

$$\tilde{p}_r = \frac{p_r}{\mathcal{B}}, \qquad \tilde{\rho} = \frac{\rho}{\mathcal{B}}, \qquad \tilde{\sigma} = \frac{\sigma}{\mathcal{B}}, \qquad \tilde{m} = m\sqrt{\mathcal{B}},$$
$$\tilde{r} = r\sqrt{\mathcal{B}}, \qquad \tilde{\omega} = \frac{\omega}{\sqrt{\mathcal{B}}}, \qquad \tilde{W} = \frac{W}{e},$$
$$\tilde{V} = \frac{V}{f}, \qquad \tilde{C}_0 = \frac{C_0}{\sqrt{\mathcal{B}}}, \qquad \tilde{C}_1 = \frac{C_1}{\mathcal{B}}, \quad \tilde{y} = y, \qquad (30)$$

where $f = \sqrt{\mathcal{B}}e$, and f and e are positive and non-null. Considering this scaling law, the stellar structure, nonradial oscillations, and tidal deformability equations keep their original form. Thus, knowing the properties of a star for a certain value of $\mathcal{B}$, the properties of another star with a different value of $\mathcal{B}'$ can be determined by considering the scale

$$\frac{\rho_c'}{\mathcal{B}'} = \frac{\rho_c}{\mathcal{B}}, \qquad M'\sqrt{\mathcal{B}'} = M\sqrt{\mathcal{B}}, \qquad R'\sqrt{\mathcal{B}'} = R\sqrt{\mathcal{B}},$$
$$\frac{\omega'}{\sqrt{\mathcal{B}'}} = \frac{\omega}{\sqrt{\mathcal{B}}}, \qquad \Lambda' = \Lambda, \qquad (31)$$

with ρ_c being the central energy density.

D. Oscillation spectrum of anisotropic strange stars

The frequency and eigenfrequency, normalized with the average density $\sqrt{M/R^3}$, versus the total mass $M/M_\odot$ are presented in the left and right panels of Fig. 1, respectively, for five values of κ. The top and bottom panels show the results for f- and p_1-modes, respectively. In the left panels, in the f-mode frequency case, we note that the curves decrease with the increment of the total mass until attaining a minimum value; after this point the curves turn counterclockwise to grow with $M/M_\odot$. In turn, in the p_1-mode

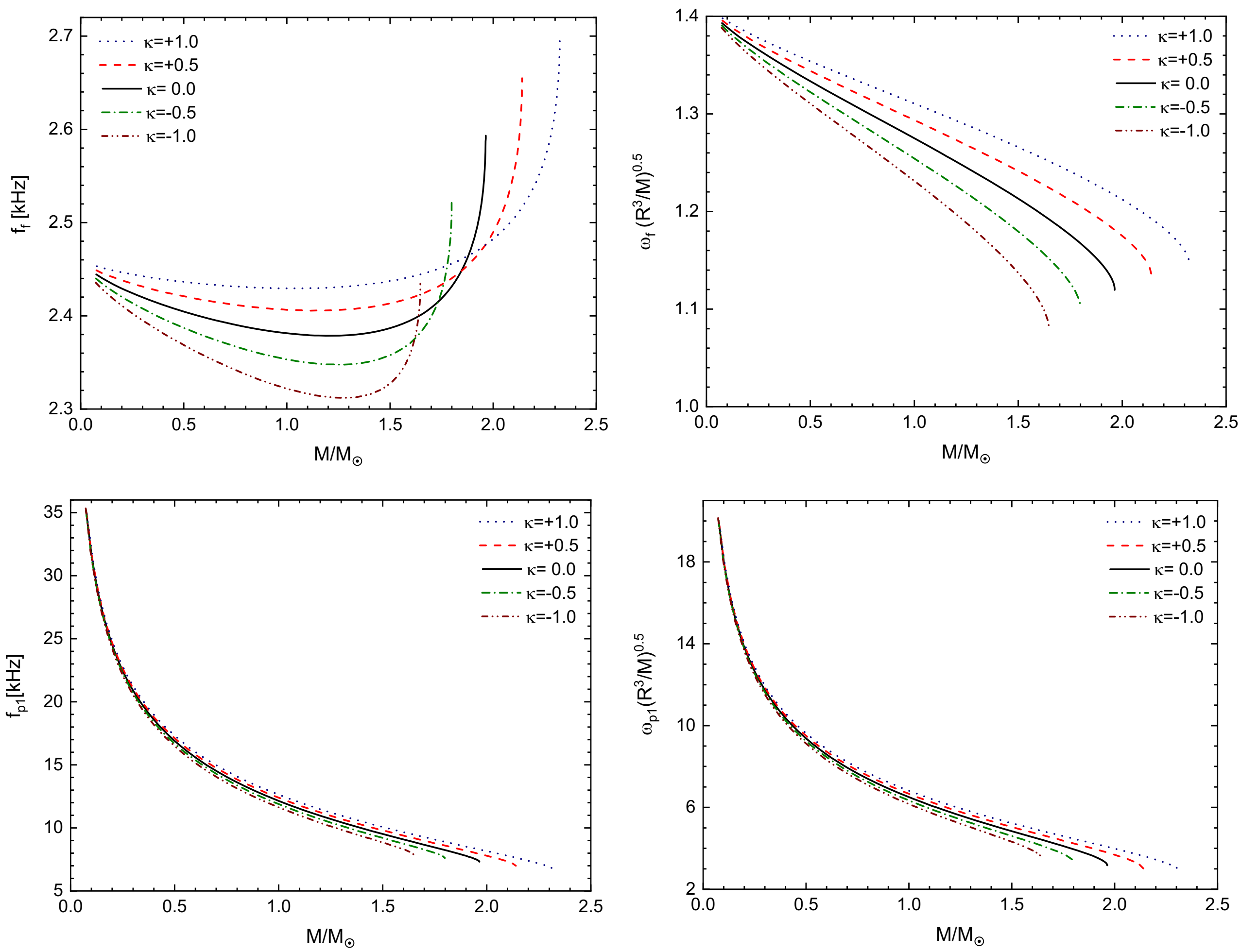

FIG. 1. Upper panels: oscillation frequency f_f (left) and normalized frequency ω_f (right) as functions of the total gravitational mass for the f-mode. Lower panels: frequencies corresponding to the p_1-mode. We use five values for the anisotropy parameter κ, where the isotropic solution is represented by the black curve. It can be observed that the f-mode frequencies increase (decrease) because of a positive (negative) anisotropy. Something similar occurs in the case of the p_1-mode frequencies; however, the impact of anisotropy is more significant only in the high-mass branch.

frequency case, we obtain that the curves decrease monotonically with the increment of $M/M_{\odot}$. In the right panels, the normalized eigenfrequencies f and in p_1 decay monotonically with the growth of $M/M_{\odot}$. Furthermore, from the figures we can also see that the anisotropy affects the pulsation mode of the fluid. We find that both the f- and p_1-mode change with κ. For greater $\kappa > 0$ (lower $\kappa < 0$), stars have a larger (lower) f_f, f_{p_1}, $\omega_f(R^3/M)^{0.5}$, and $\omega_{p_1}(R^3/M)^{0.5}$. This change in frequency is associated with the fact that the radial pressure changes with the anisotropy; see Ref. [56].

E. Tidal deformability of anisotropic strange stars

The dimensionless tidal deformability as a function of the total mass is shown in the top panel of Fig. 2 for different values of κ. These results are contrasted with the case of $\Lambda_{1.4} = 190^{+390}_{-120}$ obtained by LVC [10]. In all curves, we note that the tidal deformability decreases monotonically with the increment of the total mass. On the other hand, the effects of anisotropy on tidal deformability are also observed. We find that for a larger (lower) value of $\kappa > 0$ ($\kappa < 0$), greater (lesser) values of Λ are derived for the same mass. All of these curves are within the range of $\Lambda_{1.4}$ reported by LVC in Ref. [10]. In the bottom panel of Fig. 2, it is possible to see in more detail the effect of the anisotropic parameter on $\Lambda_{1.4}$, where the dimensionless tidal deformability undergoes a slight increment (decrement) with the increase (decrease) of the dimensionless anisotropic constant.

In the top and bottom panels of Fig. 3 we show the oscillation frequencies f_f and f_{p_1}, respectively, versus the dimensionless tidal deformability for different values of κ. These results are contrasted with the $\Lambda_{1.4} = 190^{+390}_{-120}$ reported by LVC; see Ref. [10]. In the figure, we note that the f-mode (p_1-mode) decreases (increases) monotonically with the increment of the dimensionless tidal

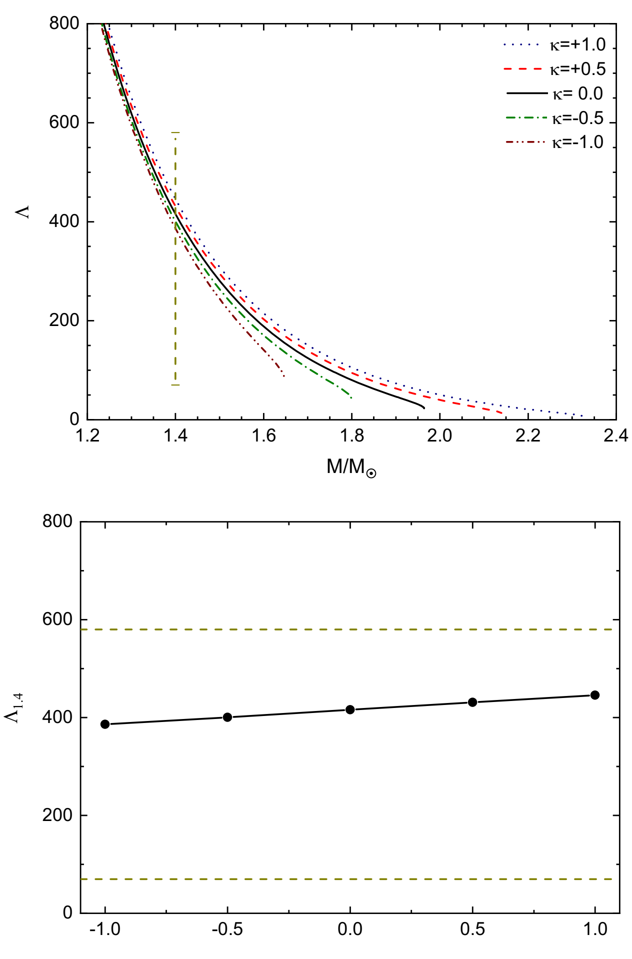

FIG. 2. Top: dimensionless tidal deformability versus the total mass for several values of κ. Bottom: $\Lambda_{1.4}$ as a function of the dimensionless anisotropic constant κ. The vertical and horizontal dashed straight lines represent $\Lambda_{1.4} = 190^{+390}_{-120}$ reported by LVC in Ref. [10].

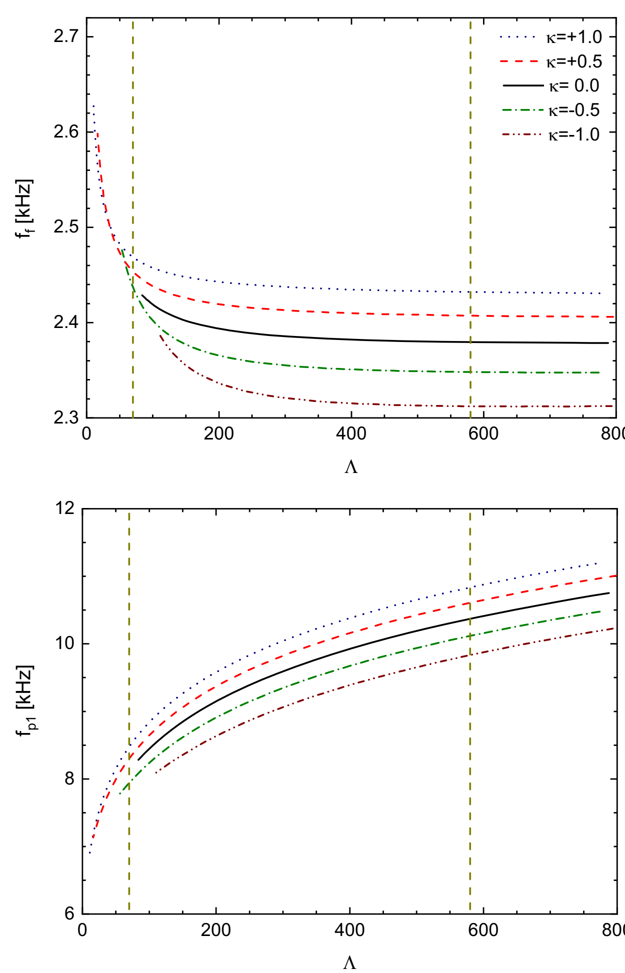

FIG. 3. The oscillation frequencies f_f and f_{p_1} versus the tidal deformability for different values of κ are plotted in the top and bottom panels, respectively. The vertical dashed straight lines mark the tidal deformability $\Lambda_{1.4} = 190^{+390}_{-120}$ from the event GW170817 estimated in Ref. [10].

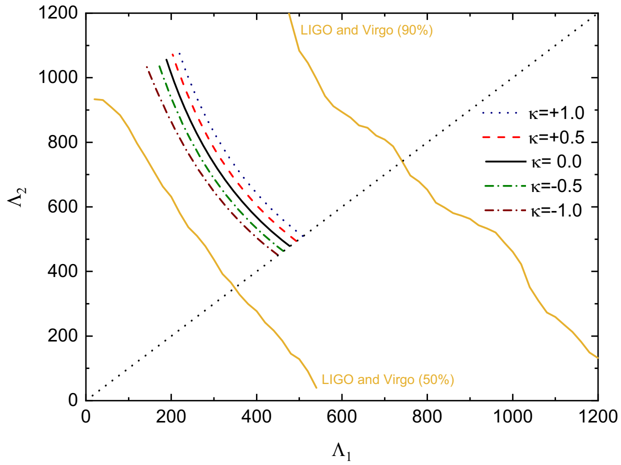

FIG. 4. Dimensionless tidal deformabilities for the components of the GW170817 event for different values of the anisotropic parameter k. The yellow line represents the LVC confidence curves [8], and the dotted diagonal line denotes the values that correspond to $\Lambda_1 = \Lambda_2$.

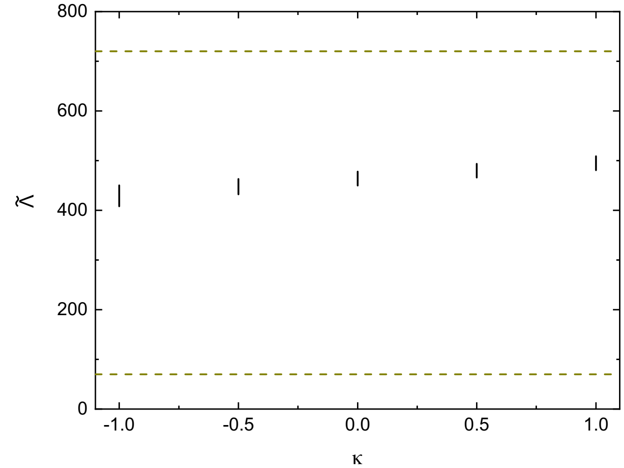

FIG. 5. $\tilde{\Lambda}$ for different values of the anisotropic parameter k. Dashed lines represent the range of $\tilde{\Lambda} = 300^{+420}_{-230}$ determined in Ref. [32].

deformability. In addition, within the interval delimited by the observation, we note that the frequency as a function of the deformability has an almost linear behavior.

The data obtained by LVC allowed the authors in Ref. [8] to establish some constraints on Λ_1 and Λ_2 which are the dimensionless tidal deformability of two compact stars in a binary system, where Λ_1 is the dimensionless tidal deformability parameter of the star with higher mass in the binary system and Λ_2 represents the same parameter of the companion star. In Fig. 4 we shown the diagram $\Lambda_1 \times \Lambda_2$, where the curves $\Lambda_1 - \Lambda_2$ are plotted first chosen a value of M_1 and determining M_2 via the chirp mass $\mathcal{M} = 1.188 M_\odot$ [8], defined by $\mathcal{M} = (M_1 M_2)^{3/5}/(M_1 + M_2)^{1/5}$. Moreover, the values considered for M_1 and M_2 are within the ranges $1.36 \le M_1/M_\odot \le 1.60$ and $1.17 \le M_2/M_\odot \le 1.36$, respectively. We also represent the lines of 50% and 90% credibility levels related to the GW170817 event established by LVC in the low-spin prior scenario. For either $\kappa > 0$ or $\kappa < 0$, we note the clear influence of the anisotropic parameter on tidal deformability. All curves derived are within the confidence lines taken from Ref. [8].

Finally, we study the dimensionless parameter $\tilde{\Lambda}$, which is measurable through the gravitational-wave signal of a binary system. $\tilde{\Lambda}$ is obtained as follows [22]:

$$\tilde{\Lambda} = \frac{16}{13} \frac{(M_1 + 12M_2) M_1^4 \Lambda_1 + (M_2 + 12M_1) M_2^4 \Lambda_2}{(M_1 + M_2)^5}. \quad (32)$$

As can be seen, it is calculated using the masses and dimensionless tidal deformability of the stars forming the binary system. Since the masses $M_1(\Lambda_1)$ and $M_2(\Lambda_2)$ are established into a particular interval of dimensionless tidal deformability in agreement with the GW170817 event, it is evident that each value of κ will produce a range for $\tilde{\Lambda}$. Thus, in Fig. 5 we show $\tilde{\Lambda}$ versus κ for anisotropic strange stars. We contrast these results with the constraint on the combined dimensionless tidal deformability reported by LVC, i.e., $\tilde{\Lambda} = 300^{+420}_{-230}$; see Ref. [32]. Note that all of the obtained values of $\tilde{\Lambda}$ are within the observational intervals.

IV. CONCLUSIONS

In this work we investigated the role of anisotropy on the fluid pulsation mode and tidal deformability of strange-quark stars. This was realized through numerically integrating the hydrostatic equilibrium, nonradial oscillation, and tidal deformability equations, which are modified to include the anisotropy effects. To describe the fluid inside the star we assumed the MIT bag model EOS and for the anisotropy factor we employed the relation $\sigma = \kappa p_r (1 - e^{-2\Psi})$.

Regarding the fluid pulsation modes, we noted that the f-mode changes considerably with the anisotropy; in contrast, the p_1-mode frequencies do not change much in the presence of anisotropy.

We also studied the compatibility of dimensionless tidal deformability of anisotropic strange stars with observational data reported by LVC from the GW170817 event. In this scenario, we noted that the results reported in this article are within the set of observational data reported by LVC. It is important to highlight that other anisotropy pressure profiles can be used in strange stars [46,56], and by analyzing their dimensionless tidal deformability we can investigate the viability of the anisotropic profile and impose some constraints using the same approach followed here. It should be noted that the deformability value increases with κ and decreases with $-\kappa$. This is in agreement with the study of polytropic stars done in Ref. [58]. However, it is in disagreement with the studies reported in Refs. [48] and [62], where the deformability profile and how it changes with anisotropy $\sigma = \kappa(\rho + p_r)(\rho + 3p_r)r^2 e^{2\Psi}/3$ was also investigated. From this, we can understand that the deformability increases or decreases with κ depending on the type of anisotropic profile employed.

Additionally, it should be noted that in some works the deformability parameter of strange stars was analyzed in different contexts. For example, in Ref. [51] this parameter was analyzed considering quark matter in the color-flavor-locked phase of color superconductivity, in Ref. [63] this factor was investigated taking into account isospin effects in strange quark matter, and in Ref. [64] tidal deformability was studied under the hypothesis that the quasiparticle model includes the nonperturbing characteristics of quantum chromodynamics in the low-density region. In the works in question, as well as in the present study, the light from the event GW170817 is used to set limits to the study of strange stars within the aforementioned contexts.

Finally, it can be mentioned that the detectability of the oscillation modes is an important issue to be considered. This detectability is strongly related with the parameters of the detectors, the most important being the sensitivity and frequency range. Moreover, it has to be considered that there are future planned upgrades for the actual operating LIGO/Virgo detector; the upgraded detector will be called LIGO Voyager [65]. In addition, it is well known that the scientific community has taken seriously the idea to build more technologically advanced gravitational-wave detectors, we can mention the third-generation detectors: Einstein Telescope [66], Cosmic Explorer [67], and NEMO [68]. The NEMO detector has a sensitivity of 10^{-24} Hz^{-1}, which is on the order of Cosmic Explorer and Einstein Telescope, but its technology primarily targets frequencies in the range of 1–4 kHz where it is possible to observe the fundamental mode. As can be seen, with all of the planned detectors, the observation of the oscillation modes of a compact star is a matter of time, and theoretical research in this direction is very important.

ACKNOWLEDGMENTS

J. D. V. A. thanks Universidad Privada del Norte and Universidad Nacional Mayor de San Marcos for the financial support of RR No. 005753–2021-R/UNMSM under the Project No. B21131781. J. M. Z. P. acknowledges financial support from the PCI program of the Brazilian agency Conselho Nacional de Desenvolvimento Científico e Tecnológico–CNPq.

APPENDIX: TIDAL DEFORMABILITY EQUATIONS FOR THE ANISOTROPIC CASE

To derive the differential equations used to investigate the dimensionless tidal deformability for the anisotropic case, we start by considering the perturbed field equation

$$\delta G^{\mu}_{\varphi} = 8\pi \delta T^{\mu}_{\varphi}, \tag{A1}$$

and, following Thorne and Campolattaro's work [69], we use the linear perturbation of the background metric tensor of the form

$$g^{(*)}_{\alpha\beta} = g_{\alpha\beta} + h_{\alpha\beta}, \tag{A2}$$

where $g_{\alpha\beta}$ and $h_{\alpha\beta}$ are the unperturbed metric tensor and the linearized perturbed metric, respectively. With these specializations, $h_{\alpha\beta}$ can be written as [69,70]

$$h_{\alpha\beta} = \mathrm{diag}[He^{2\Phi}, He^{2\Psi}, r^2 K, r^2 K \sin^2\theta] Y_{\ell m}, \tag{A3}$$

where $H = H(r)$ and $K = K(r)$ depend on the radial coordinate, and $Y_{\ell m} = Y_{\ell m}(\theta, \phi)$ is a function of the angular coordinates.

Expanding the fluid perturbation variables in terms of $Y_{\ell m}$, from the perturbed field equation (A1) we find

$$\left[e^{-2\Psi}\left(K'' - K'\Psi' - \frac{H'}{r} + \frac{3K'}{r} - \frac{H}{r^2} + \frac{2H}{r}\Psi'\right) - \frac{H\ell(\ell+1)}{2r^2} + \frac{K}{r^2} - \frac{K\ell(\ell+1)}{2r^2}\right] Y_{\ell m} = -8\pi\delta\rho, \tag{A4}$$

$$\left[e^{-2\Psi}\left(K'\Phi' - 2H\frac{\Phi'}{r} - \frac{H'}{r} + \frac{K'}{r} - \frac{H}{r^2}\right) + \frac{K}{r^2} + \frac{\ell(\ell+1)(H-K)}{2r^2}\right] Y_{\ell m} = 8\pi\delta p_r, \tag{A5}$$

$$\begin{aligned}&\left[rHe^{2\Phi}\Psi'\Phi' - rHe^{2\Phi}\Phi'^2 - rHe^{2\Phi}\Phi'' + \frac{re^{2\Phi}H'\Psi'}{2} - \frac{3}{2}re^{2\Phi}H'\Phi' - \frac{re^{2\Phi}H''}{2} - \frac{re^{2\Phi}K'\Psi'}{2}\right.\\ &\left.+\frac{re^{2\Phi}K'\Phi'}{2} + \frac{re^{2\Phi}K''}{2} + He^{2\Phi}\Psi' - He^{2\Phi}\Phi' - H'e^{2\Phi} + K'e^{2\Phi}\right]\frac{e^{-2(\Psi+\Phi)}}{r} Y_{\ell m} = 8\pi\delta p_t,\end{aligned} \tag{A6}$$

$$\left[\frac{H\Phi'}{r^2} + \frac{H'}{2r^2} - \frac{K'}{2r^2}\right]\partial_\theta Y_{\ell m} = 0. \tag{A7}$$

Substituting Eq. (A7), where $K' = 2H\Phi' + H'$ and $K'' = 2H'\Phi' + 2H\Phi'' + H''$, into the difference between Eqs. (A4) and (A5) and into Eq. (A6), we have, respectively,

$$\begin{aligned} &-2Y_{\ell m}e^{-2\Psi}H\Psi'\Phi' - Y_{\ell m}e^{-2\Psi}H'\Psi' + 2Y_{\ell m}e^{-2\Psi}H'\Phi' + 2Y_{\ell m}e^{-2\Psi}H\Phi'' + Y_{\ell m}e^{-2\Psi}H'' + \frac{2H}{r}Y_{\ell m}e^{-2\Psi}\Psi' \\ &+\frac{6H}{r}Y_{\ell m}e^{-2\Psi}\Phi' + \frac{2H'}{r}Y_{\ell m}e^{-2\Psi} - \frac{H\ell(\ell+1)Y_{\ell m}}{r^2} - 2Y_{\ell m}e^{-2\Psi}H\Phi'^2 - Y_{\ell m}e^{-2\Psi}\Phi'H' = -8\pi(\delta\rho + \delta p_r), \end{aligned} \tag{A8}$$

$$\frac{H}{r}e^{-2\Psi}Y_{\ell m}(\Psi' + \Phi') = 8\pi\delta p_t. \tag{A9}$$

For the perturbation of the radial pressure $p_r = p_r(p_t, \Psi)$, we have

$$\delta p_r = \frac{\partial p_r}{\partial p_t}\delta p_t, \tag{A10}$$

where it is considered that $\delta\Psi = 0$. In addition, $\delta\rho$ is defined by considering the equation of state $\rho = \rho(p_r)$. In this way, by replacing Eqs. (A8) and (A9) we obtain

$$H'' + C_0H' + C_1H = 0, \tag{A11}$$

where the functions $C_0 = C_0(r)$ and $C_1 = C_1(r)$ are calculated as functions of the background quantities as follows:

$$C_0 = \frac{2m}{r^2}e^{2\Psi} + 4\pi e^{2\Psi}(p_r - \rho)r + \frac{2}{r}, \tag{A12}$$

$$\begin{aligned} C_1 = {}& 4\pi e^{2\Psi}\left[4\rho + 4p_r + 4p_t + \frac{p_r + \rho}{Ac_s^2}(c_s^2 + 1)\right] \\ &- \frac{\ell(\ell+1)}{r^2}e^{2\Psi} - 4\Phi'^2, \end{aligned} \tag{A13}$$

with $c_s^2 = \frac{dp_r}{d\rho}$ and $A = \frac{dp_t}{dp_r}$.

[1] B. P. Abbott *et al.*, Observation of Gravitational Waves from Binary Black Hole Merger, Phys. Rev. Lett. **116**, 061102 (2016).

[2] B. P. Abbott *et al.*, GW151226: Observation of Gravitational Waves from a 22-Solar-Mass Binary Black Hole Coalescence, Phys. Rev. Lett. **116**, 241103 (2016).

[3] B. P. Abbott *et al.*, Tests of General Relativity with GW150914, Phys. Rev. Lett. **116**, 221101 (2016); **116**, 221101(E) (2016); **121**, 129902(E) (2018).

[4] B. P. Abbott *et al.*, GW170104: Observation of a 50-Solar-Mass Binary Black Hole Coalescence at Redshift 0.2, Phys. Rev. Lett. **118**, 221101 (2017).

[5] B. P. Abbott *et al.*, GW170814: A Three-Detector Observation of Gravitational Waves from a Binary Black Hole Coalescence, Phys. Rev. Lett. **119**, 141101 (2017).

[6] B. P. Abbott *et al.*, GW170608: Observation of a 19 solar-mass binary black hole coalescence, Astrophys. J. Lett. **851**, L35 (2017).

[7] B. P. Abbott *et al.*, Astrophysical implications of the binary black hole merger GW150914, Astrophys. J. Lett. **818**, L22 (2016).

[8] B. P. Abbott *et al.*, GW170817: Observation of Gravitational Waves from a Binary Neutron Star Inspiral, Phys. Rev. Lett. **119**, 161101 (2017).

[9] B. P. Abbott *et al.*, Multi-messenger observational of a binary neutron star merger, Astrophys. J. Lett. **848**, L12 (2017).

[10] B. P. Abbott *et al.*, GW170818: Measurements of Neutron Star Radii and Equation of State, Phys. Rev. Lett. **121**, 161101 (2018).

[11] S. Turck-Chièze and I. Lopes, Solar-stellar astrophysics and dark matter, Res. Astron. Astrophys. **12**, 1107 (2012).

[12] I. Lopes and J. Silk, Dark matter imprint on ^{8}B neutrino spectrum, Phys. Rev. D **99**, 023008 (2019).

[13] I. D. Saltas and I. Lopes, Obtaining Precision Constraints on Modified Gravity with Helioseismology, Phys. Rev. Lett. **123**, 091103 (2019).

[14] G. J. Olmo, D. Rubiera-Garcia, and A. Wojnar, Stellar structure models in modified theories of gravity: Lessons and challenges, Phys. Rep. **876**, 1 (2020).

[15] I. P. Lopes, Nonradial adiabatic oscillations of stars. Mode classification of acoustic-gravity waves, Astron. Astrophys. **373**, 916 (2001).

[16] I. Lopes, A new look at the Eckart-Scuflaire-Osaki classification scheme of stellar oscillations, Astrophys. J. **542**, 1071 (2000).

[17] G. Miniutti, J. A. Pons, E. Berti, L. Gualtieri, and V. Ferrari, Non-radial oscillation modes as a probe of density discontinuities in neutron stars, Mon. Not. R. Astron. Soc. **338**, 389 (2003).

[18] A. Passamonti, M. Bruni, L. Gualtieri, and C. F. Sopuerta, Coupling of radial and nonradial oscillations of relativistic

stars: Gauge-invariant formalism, Phys. Rev. D **71**, 024022 (2005).
[19] A. Passamonti, M. Bruni, L. Gualtieri, A. Nagar, and C. F. Sopuerta, Coupling of radial and axial nonradial oscillations of compact stars: Gravitational waves from first-order differential rotation, Phys. Rev. D **73**, 084010 (2006).
[20] G. J. Savonije, Non-radial oscillations of the rapidly rotating Be star HD 163868, Astron. Astrophys. **469**, 1057 (2007).
[21] C. V. Flores, Z. B. Hall, and P. Jaikumar, Nonradial oscillation modes of compact stars with a crust, Phys. Rev. C **96**, 065803 (2017).
[22] E. E. Flanagan and T. Hinderer, Constraining neutron star tidal Love numbers with gravitational wave detectors, Phys. Rev. D **77**, 021502(R) (2008).
[23] T. Binnington and E. Poisson, Relativistic theory of tidal Love numbers, Phys. Rev. D **80**, 084018 (2009).
[24] T. Hinderer, Tidal love numbers of neutron stars, Astrophys. J. **677**, 1216 (2008).
[25] S. Postnikov, M. Prakash, and J. M. Lattimer, Tidal Love numbers of neutron and self-bound quark stars, Phys. Rev. D **82**, 024016 (2010).
[26] T. Damour and A. Nagar, Relativistic tidal properties of neutron stars, Phys. Rev. D **80**, 084035 (2009).
[27] A. I. Sokolov, Phase transitions in a superfluid neutron liquid, Sov. Phys. JETP **52**, 575 (1980), http://www.jetp.ras.ru/cgi-bin/dn/e_052_04_0575.pdf.
[28] R. F. Sawyer, Condensed π^- Phase in Neutron-Star Matter, Phys. Rev. Lett. **29**, 382 (1972).
[29] R. Ruderman, Pulsars: Structure and dynamics, Annu. Rev. Astron. Astrophys. **10**, 427 (1972).
[30] H. Heiselberg and M. H. Jensen, Phases of dense matter in neutron stars, Phys. Rep. **328**, 237 (2000).
[31] R. Kippenhahn and A. Weigert, *Stellar Structure and Evolution* (Springer, Berlin, 1990).
[32] B. P. Abbott *et al.*, Properties of the Binary Neutron Star Merger GW170817, Phys. Rev. X **9**, 011001 (2019).
[33] R. C. Tolman, Static solution of Einstein's field equation for spheres of fluid, Phys. Rev. D **55**, 364 (1939).
[34] J. R. Oppenheimer and G. Volkoff, On massive neutron cores, Phys. Rev. D **55**, 374 (1939).
[35] R. L. Bowers and E. P. T. Liang, Anisotropic spheres in general relativity, Astrophys. J. **188**, 657 (1974).
[36] P. N. McDermott, H. M. Van Horn, and J. F. Scholl, Nonradial g-mode oscillations of warm neutron stars, Astrophys. J. **268**, 837 (1983).
[37] L. Lindblom and R. J. Splinter, The accuracy of the relativistic Cowling approximation, Astrophys. J. **348**, 198 (1990).
[38] C. Vásquez Flores and G. Lugones, Discriminating hadronic and quark stars through gravitational waves of fluid pulsation modes, Classical Quantum Gravity **31**, 155002 (2014).
[39] H. Sotani, N. Yasutake, T. Maruyama, and T. Tatsumi, Signatures of hadron-quark mixed phase in gravitational waves, Phys. Rev. D **83**, 024014 (2011).
[40] S. Yoshida and Y. Kojima, Accuracy of the relativistic Cowling approximation in slowly rotating stars, Mon. Not. R. Astron. Soc. **289**, 117 (1997).
[41] A. Stavridis, A. Passamonti, and K. Kokkotas, Nonradial oscillations of slowly and differentially rotating compact stars, Phys. Rev. D **75**, 064019 (2007).
[42] S. Boutloukos and H. P. Nollert, Eigenmode frequency distribution of rapidly rotating neutron stars, Phys. Rev. D **75**, 043007 (2007).
[43] L. Samuelsson and N. Andersson, Neutron star asteroseismology. Axial crust oscillations in the Cowling approximation, Mon. Not. R. Astron. Soc. **374**, 256 (2007).
[44] D. D. Doneva and S. S. Yazadjiev, Nonradial oscillations of anisotropic neutron stars in the Cowling approximation, Phys. Rev. D **85**, 124023 (2012).
[45] J. D. V. Arbañil, C. H. Lenzi, and M. Malheiro, Fluid pulsation modes from strange stars in a higher-dimensional space-time, Phys. Rev. D **102**, 084014 (2020).
[46] E. J. Aquino Curi, L. B. Castro, C. V. Flores, and C. H. Lenzi, Non-radial oscillations and global stellar properties of anisotropic compact stars using realistic equations of state, Eur. Phys. J. C **82**, 527 (2022).
[47] T. Hinderer, B. D. Lackey, R. N. Lang, and J. S. Read, Tidal deformability of neutron stars with realistic equations of state and their gravitational wave signatures in binary inspiral, Phys. Rev. D **81**, 123016 (2010).
[48] B. Biswas and S. Bose, The tidal deformability of an anisotropic compact star: Implications of GW170817, Phys. Rev. D **99**, 104002 (2019).
[49] A. Rahmansyah, A. Sulaksono1, A. B. Wahidin, and A. M. Setiawan, Anisotropic neutron stars with hyperons: Implication of the recent nuclear matter data and observations of neutron stars, Eur. Phys. J. C **80**, 769 (2020).
[50] E. P. Zhou, X. Zhou, and A. Li, Constraints on interquark interaction parameters with GW170817 in a binary strange star scenario, Phys. Rev. D **97**, 083015 (2018).
[51] O. Lourenço, C. H. Lenzi, M. Dutra, E. J. Ferrer, V. de la Incera, L. Paulucci, and J E. Horvath, Tidal deformability of strange stars and the GW170817 event, Phys. Rev. D **103**, 103010 (2021).
[52] Q. Wang, C. Shi, and H. S. Zong, Nonstrange quark stars from an NJL model with proper-time regularization, Phys. Rev. D **100**, 123003 (2019); **100**, 129903(E) (2019).
[53] C. M. Li, S. Y. Zuo, Y. Yan, Y. P. Zhao, F. Wang, Y. F. Huang, and H. S. Zong, Strange quark stars within proper time regularized $(2+1)$-flavor NJL model, Phys. Rev. D **101**, 063023 (2020).
[54] E. Witten, Cosmic separation of phases, Phys. Rev. D **30**, 272 (1984).
[55] E. Farhi and R. L. Jaffe, Strange matter, Phys. Rev. D **30**, 2379 (1984).
[56] J. D. V. Arbañil and M. Malheiro, Radial stability of anisotropic strange quark stars, J. Cosmol. Astropart. Phys. 11 (2016) 012.
[57] D. Horvat, S. Ilijic, and A. Marunociv, Radial pulsations and stability of anisotropic stars with quasi-local equation of state, Classical Quantum Gravity **28**, 025009 (2011).
[58] J. D. V. Arbañil and G. Panotopoulos, Tidal deformability and radial oscillations of anisotropic polytropic spheres, Phys. Rev. D **105**, 024008 (2022),

[59] V. Folomeev and V. Dzhunushaliev, Magnetic fields in anisotropic relativistic stars, Phys. Rev. D **91**, 044040 (2015).

[60] H. O. Silva, C. F. B. Macedo, E. Berti, and L. C. B. Crispino, Slowly rotating anisotropic neutron stars in general relativity and scalar-tensor theory, Classical Quantum Gravity **32**, 145008 (2015).

[61] N. K. Glendenning, *Compact Stars: Nuclear Physics, Particle Physics and General Relativity* (Springer-Verlag, Berlin, 1997).

[62] H. C. Das, I-Love-C relation for an anisotropic neutron star, Phys. Rev. D **106**, 103518 (2022).

[63] B. L. Li, Y. Yan, and J. L. Ping, Tidal deformabilities and radii of strange quark stars, Phys. Rev. D **104**, 043002 (2021).

[64] J.-F. Xu, C.-J. Xia, Z.-Y. Lu, G.-X. Peng, and Y.-P. Zhao, Symmetry energy of strange quark matter and tidal deformability of strange quark stars, Nucl. Sci. Tech. **33**, 143 (2022).

[65] R. X. Adhikari *et al.*, A cryogenic silicon interferometer for gravitational-wave detection, Classical Quantum Gravity **37**, 165003 (2020).

[66] M. Punturo *et al.*, The Einstein Telescope: A third-generation gravitational wave observatory, Classical Quantum Gravity **27**, 194002 (2010).

[67] R. David *et al.*, Cosmic Explorer: The U.S. Contribution to gravitational-wave astronomy beyond LIGO, Bull. Am. Astron. Soc. **51**, 7 (2019), https://baas.aas.org/pub/2020n7i035/release/1.

[68] K. Ackley *et al.*, Neutron Star Extreme Matter Observatory: A kilohertz-band gravitational-wave detector in the global network, Publ. Astron. Soc. Aust. **37**, e047 (2020).

[69] K. S. Thorne and A. Campolattaro, Non-radial pulsation of general-relativistic stellar models I. Analytic analysis for $\ell \geq 2$, Astrophys. J. **149**, 591 (1967).

[70] T. Regge and J. A. Wheeler, Stability of a Schwarzschild singularity, Phys. Rev. **108**, 1063 (1957).